Utrecht University

Royal Netherlands Institute for Sea Research (NIOZ)

Bachelor thesis

Experiments on surface waves

Author:
Vera van Bergeijk

Supervisors:
Leo Maas
Sander van Oers

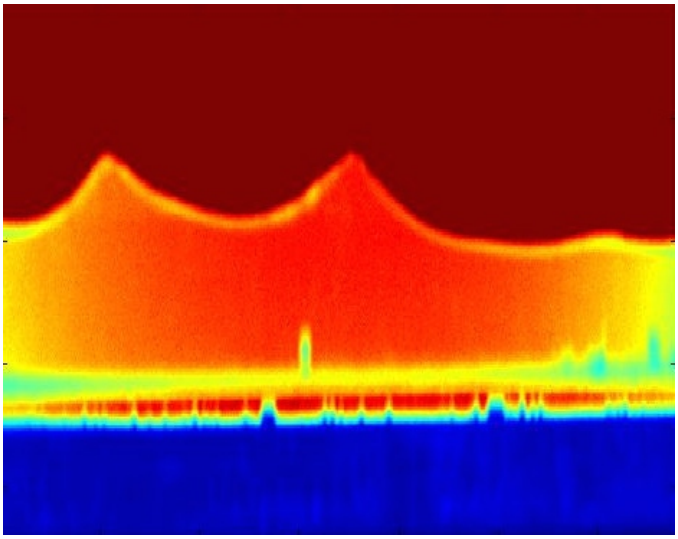

June 30, 2015

Abstract

In this thesis laboratory experiments were done to determine the influence of the water depth, forcing frequency and topography of the water tank on surface waves and resonant frequencies. The most interesting topic of this thesis is the change in the topography of water tank, which was done by changing the tank length, putting a partitioning wall at a tilt and adding a slope or mountain. The partioning wall with a tilt increases the resonant frequencies with increasing angle of tilt and with increasing order of resonance. A slope was added to the tank to determine the influence on the frequency domains of the solitons and the surface elevation. For a small water depth no change in surface elevation was observed, but at a higher depth the surface elevation became larger for high forcing frequencies. Adding a mountain to the water tank lowers the resonant frequencies, that decrease the most in the middle of the water tank. Importantly it was found that the change in the location of node for the first resonant frequency was discrete and not symmetric contrary to the expectation of a linear and symmetric change.

Contents

1 Introduction

Surface waves are waves that propagate along the water edge, the interface between the water and the air. Surface waves have been the subject of research for decades, but still a lot can be learned about surface waves. Surface waves travelling in the ocean can range in size from small ripples to tsunamis. An interesting case of surface waves in the ocean is the case of huge waves, called freak waves, which can occur out of nowhere. For a long time people believed these freak waves were fiction, but on 1 January 1995 the first freak wave was recorded by a measuring instrument at the Drauoner platform. The so-called *New Year Wave or the Draupner Wave* was close to 25.6 meters high [1]. These spontaneous occurring surface waves are dangerous for ships, because they are not built for this strange type of waves. How these freak waves arise is still not understood.
Surface waves also propagate along the interface of two fluids with different densities. These waves are called interfacial waves and give rise to another interesting phenomenon called dead water. Dead water was first described by Fridtjof Nansen in August 1893 [2]. When a layer of fresh water is on top of the salt water of the ocean and these layers don't mix, a ship can be slowed down or even be stopped completely. The power of the ship leads to interfacial waves and turbulence between the two layers, leaving no power for the ship's transport .

So there are some interesting phenomena related to surface waves, but not all are understood. Experiments on surface waves hopefully will help solving these problems. Experiments on the open ocean are expensive and difficult, since not all parameters can be controlled. Contrary to laboratory experiments where one can control almost all conditions. The parameters can be varied one by one to determine the influence of an individual parameter only. There is a large variety of surface waves, but this laboratory experiment focuses on standing waves and solitary waves. This thesis will elaborate on the following research question:

What influence do the water depth, forcing frequency and topography of the water tank have on surface waves and resonant frequencies?

The laboratory experiments took place at the Royal Netherlands Institute for Sea Research (NIOZ). Not only the forcing frequency was changed in this experiment, also different types of forcing were used. The influence of the topography of the water tank was investigated by changing the length of the water tank and by placing slopes inside the tank. The experiments of changing the topography are particularly interesting because this is the first time this manner of experiments has been performed at the NIOZ.

2 Theory

2.1 Derivation of the dispersion relation

In this thesis only 2-dimensional waves are discussed: the wave is only moving in the x-direction while the water height changes in the z-direction. The derivation of the dispersion relation is based on the chapter on linear small amplitude wave theory in the book 'An introduction to hydrodynamics and water waves' by Le Méhauté [3]. In the linear small amplitude wave theory the non-linear convective inertia terms are considered to be small. Also the motion is irrotational.

2.1.1 Notation and continuity

The symbols used are (p) for the pressure, (ρ) for the density and the gravitational acceleration is given by $g = 9.81\ m/s^2$. The wave number k is defined as $k = 2\pi/\lambda$, where λ is the wave length. The water depth is denoted by H. The space variables x and z are zero at the water surface as shown in figure 1. The symbol η is used for the *free surface*. The velocity $\vec{V}$ is defined as $\vec{V} = (u, w) = (-\partial\phi/\partial x, -\partial\phi/\partial z)$ with $\phi(x, z, t)$ is the *single-valued velocity potential function*.

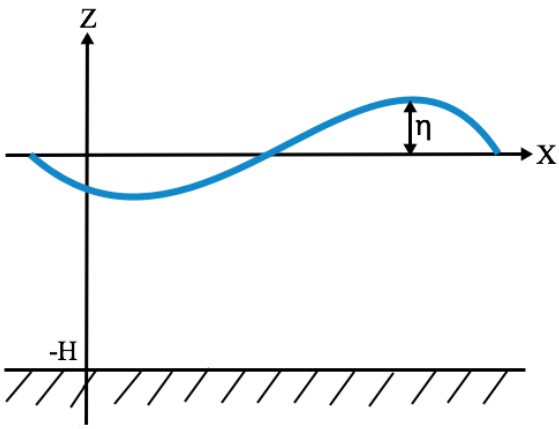

Figure 1: The notation used to describe the water surface. The spacevariable z is zero at the water edge. The water depth is denoted by H and the symbol η is used for the free surface.

The momentum equation is given by the following form of the Bernoulli equation:

$$-\frac{\partial\phi}{\partial t} + \frac{1}{2}V^2 + \frac{p}{\rho} + gz = f(t). \tag{1}$$

When the velocity V is replaced by the velocity potential function ϕ the momentum equation becomes

$$-\frac{\partial\phi}{\partial t} + \frac{1}{2}[(\frac{\partial\phi}{\partial x})^2 + (\frac{\partial\phi}{\partial z})^2] + \frac{p}{\rho} + gz = f(t). \tag{2}$$

The function f(t) may depend on the time t, but not on the space variables x and z.

The *continuity equation* is given by the following equation:

$$\nabla \cdot \vec{V} = \frac{\partial u}{\partial x} + \frac{\partial w}{\partial z} = \nabla^2\phi = 0. \tag{3}$$

2.1.2 General boundary conditions

At a fixed boundary, the velocity normal to the surface needs to be zero. So at the horizontal bottom the vertical velocity is zero.

$$w|_{z=-H} = -\frac{\partial \phi}{\partial z}\bigg|_{z=-H} = 0. \tag{4}$$

At the free surface the time derivative of the local water height $z = \eta(x,t)$ is called the free surface equation

$$\frac{dz}{dt} = \frac{\partial \eta}{\partial t} + \frac{\partial \eta}{\partial x}\frac{dx}{dt}. \tag{5}$$

Using the values $dx/dt = u = -\partial\phi/\partial x$ and $dz/dt = w = -\partial\phi/\partial z$ equation 5 becomes

$$\frac{\partial \phi}{\partial z}\bigg|_{z=\eta} = -\frac{\partial \eta}{\partial t} + \frac{\partial \phi}{\partial x}\bigg|_{z=\eta}\frac{\partial \eta}{\partial x}. \tag{6}$$

This equation is called *the free surface kinematic condition.*

The *dynamic condition* is obtained by considering the pressure p as constant. The momentum equation becomes

$$-\frac{\partial \phi}{\partial t} + \frac{1}{2}[(\frac{\partial \phi}{\partial x})^2 + (\frac{\partial \phi}{\partial z})^2] + g\eta = f(t). \tag{7}$$

2.1.3 The Cauchy-Poisson condition

In very slow motion the convective term is neglected and the Bernoulli equation is written as

$$-\frac{\partial \phi}{\partial t} + \frac{p}{\rho} + gz = f(t), \tag{8}$$

which at the free surface becomes

$$-\frac{\partial \phi}{\partial t}\bigg|_{z=\eta} + g\eta = 0. \tag{9}$$

When the function f(t) and any additive constant can be included in the value of $\partial\phi/\partial t$, this results in

$$\eta = \frac{1}{g}\frac{\partial \phi}{\partial t}. \tag{10}$$

The component of the slope of the free surface $\partial\eta/\partial x$ is small in case of slow motion, so in the kinematic boundary condition the term $(\partial\phi/\partial x)(\partial\eta/\partial x)$ can be neglected.

$$\frac{\partial\eta}{\partial t} = -\left.\frac{\partial\phi}{\partial z}\right|_{z=0}. \tag{11}$$

The derivative of η with respect to the time t in the dynamic condition gives

$$\frac{\partial\eta}{\partial t} = \left.\frac{1}{g}\frac{\partial^2\phi}{\partial t^2}\right|_{z=0}. \tag{12}$$

When $\partial\eta/\partial t$ is eliminated, the Cauchy-Poisson condition at the free surface is obtained

$$\left[\frac{\partial\phi}{\partial z} + \frac{1}{g}\frac{\partial^2\phi}{\partial t^2}\right]_{z=0} = 0. \tag{13}$$

2.1.4 General solution

The continuity equation 3 can be solved using separation of variables when ϕ is given by the product of the functions of the horizontal component $U(x)$, the vertical component $P(z)$ and the time $f(t)$. The function $f(t)$ can be written as $f(t) = cos[\omega t + \epsilon]$ where ω is the frequency given by $\omega = 2\pi/T$ with T the wave period. Inserting $\phi = U(x) \cdot P(z) \cdot cos[\omega t + \epsilon]$ in the continuity equation leads to

$$-\frac{\partial^2 U/\partial x^2}{U(x)} = \frac{d^2P/dz^2}{P(z)}. \tag{14}$$

The left-hand side only depends on x, while the right-hand side only depends on z. The only way a function of x and a function of z can be the same is when they are equal to a constant. The constant k is chosen to be real and so k^2 is always positive. Equation 14 becomes

$$(\frac{d^2}{dz^2} - k^2)P(z) = 0, \tag{15}$$

$$(\frac{d^2}{dx^2} + k^2)U = 0, \tag{16}$$

where the last equation is the well-known *Helmholtz equation.* Equation 15 is easily integrated, giving the general solution

$$P = Ae^{kz} + Be^{-kz}. \tag{17}$$

The boundary condition at the bottom (equation 4) gives for any fixed value of x and t:

$$\frac{dP}{dz}|_{z=-H} = 0.$$

Applying to the solution for $P(z)$ results in $Ae^{-kH} = Be^{kH} = D/2$ where the constant D is used for convenience. Multiply $P(z)$ by $e^{-kH}e^{kH}$ yields

$$P(z) = \frac{D}{2}(e^{k(z+H)} + e^{-k(z+H)}) = D\cosh[k(z+H)]. \tag{18}$$

The expression of ϕ becomes after substituting $P(z)$

$$\phi = D\cosh[k(z+H)] \cdot U(x) \cdot \cos[\omega t + \epsilon]. \tag{19}$$

The Cauchy-Poisson condition at the free surface

$$[\frac{\partial \phi}{\partial z} + \frac{1}{g}\frac{\partial^2 \phi}{\partial t^2}]_{z=0} = 0, \tag{20}$$

results in

$$w^2 = gk\tanh(kH), \tag{21}$$

which leads to the *dispersion relation*

$$\omega = \pm\sqrt{gk\tanh(kH)}. \tag{22}$$

In the shallow water limit the water depth H is small, so $\tanh(kH) \simeq kH$. The dispersion relation in the shallow water limit is given by

$$\omega = \pm\sqrt{gH}k. \tag{23}$$

2.2 Progressive waves

Progressive waves are travelling waves that do not change for an observer that is travelling at the same speed and in the same direction as the wave.[3] Two waves travelling with the same speed and amplitude, but in opposite directions, can interfere and create a standing wave. For a progressive wave the solution of the Helmholtz equation 16 is

$$U(x) = Ae^{ikx} + Be^{ikx}. \tag{24}$$

The velocity potential function can be written as

$$\phi(x,z,t) = c^+\phi^+ + c^-\phi^-, \tag{25}$$

with c^+ and c^- constants which depend on the boundary equation and $\phi^\pm$ is given by

$$\phi^\pm = ce^{\pm ikx}\cosh[k(z+H)] \cdot \cos[\omega t + \epsilon]. \tag{26}$$

2.3 Evanescent waves

Evanescent waves are localized waves that are formed at a boundary. The intensity of these waves decays exponentially with the distance from the boundary at which they are formed. Evanescent waves are the solutions of equations 15 and 16 where instead of choosing the constant real, the equations are equal to the constant κ which can be complex.

$$-\frac{U(x)''}{U(x)} = \frac{P(z)"}{P(z)} = -\kappa^2. \tag{27}$$

The general solution for P(z) becomes now

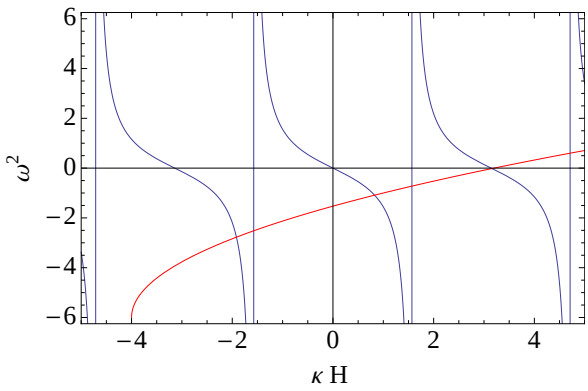

Figure 2: The dispersion relation for evanescent waves leads to several options of the wave number κ

$$P(z) = A'e^{i\kappa z} + Be'^{-i\kappa z}. \tag{28}$$

Using the boundary condition 4 and multiplying P(z) this time by $e^{i\kappa z}e^{-i\kappa z}$ the expression for P(z) becomes

$$P(z) = D' \cos[\kappa(z + H)], \tag{29}$$

where the constant $D' = A'e^{-i\kappa H} = B'e^{i\kappa H}$ is again used for a convience. When κ is introduced, the Helmholtz equation 16 becomes

$$(\frac{\partial^2}{\partial x^2} - \kappa^2)U(x) = 0. \tag{30}$$

This equation is solved easily

$$U(x) = Ae^{-\kappa x} + Be^{-\kappa x}. \tag{31}$$

Inserting $U(x)$ and $P(z)$ in the expression for the velocity potential function ϕ

$$\phi(x, z, t) = (C_1 e^{-\kappa x} + C_2 e^{\kappa x}) \cos[\kappa(z + H)] \cdot \cos[\omega t + \epsilon], \tag{32}$$

where C_1 en C_2 are constants which are determined by the boundary conditions.

The Cauchy-Poisson condition at the free surface 13 leads to the dispersion relation for evanescent waves

$$\omega^2 = -\kappa_n g \tan[\kappa_n H]. \tag{33}$$

The indexes n are added to the complex wave number κ_n because there exist several possibilities for the complex wave number as shown in figure 2. The formula $\tan[\kappa H]$ is plotted in blue and in red is a possible line for the frequency ω^2 plotted. The lines have multiple points of intersection, which lead to multiple possibilities of the complex wave number κ.

The velocity potential function for evanescent waves can be written as

$$\phi = \sum_{j=1} c_j^+ \phi_n^+ + c_j^- \phi_n^-, \tag{34}$$

where $c_j^\pm$ is determined by the boundary conditions and $\phi_n^\pm$ is given by

$$\phi_n^\pm = e^{\pm\kappa_n x} cos[\kappa_n(z+H)] \cdot \cos[\omega t + \epsilon]. \tag{35}$$

2.4 The velocity potential in a water tank with length L

In this section the lateral boundary conditions are applied to obtain an expression for the wave number and to solve the velocity potential function. The lateral boundary condition says that no water can flow across a boundary:

$$\frac{\partial \phi}{\partial n} = 0. \tag{36}$$

The total velocity potential for progressive and evanescent waves is

$$\phi = c^+\phi^+ + c^-\phi^- + \sum_{j=1} c_j^+ \phi_n^+ + c_j^- \phi_n^-. \tag{37}$$

As will be proven in this section there only exist progressive waves for a water tank with vertical walls, but when a slope is added to one side of the water tank evanescent waves will be present. This prove is given by trying to solve the velocity potential function for the absence of evanescent waves ($c_j^\pm = 0$) as given by equation 25. When the velocity potential function can be solved for progressive waves only, there are nog evanescent waves present. If no velocity potential function can be found, then there have to be evanescent waves.

2.4.1 A water tank with vertical walls

For a water tank with vertical walls (90° with bottom) the flow in the x-direction at x=0 and x=L has to be zero.

$$\left.\frac{\partial \phi}{\partial x}\right|_{x=L} = \left.\frac{\partial \phi}{\partial x}\right|_{x=0} = 0. \tag{38}$$

At x=0 the lateral boundary condition leads to $c^+ = c^-$. The lateral boundary condition at x=L leads to $e^{ikL} = e^{-ikL}$. This relation only holds if $kL = \pi n$ with n an integer. So the wave number k becomes $k = \pi n/L$ and the velocity potential function becomes

$$\phi = A\cos[\omega t + \epsilon]\cosh[\frac{\pi n}{L}(z+H)]\cos[\frac{\pi n}{L}x]. \tag{39}$$

The velocity potential function is solved with only the use of progressive waves, which means that no evanescent waves are present in a water tank with vertical walls.

2.4.2 A water tank with one slope

The slope is placed at the left end of the water tank and the notation used is shown in figure 3. In this figure can be seen that $\tan(\theta) = \Delta L/h = x_0/z$, so x_0 satisfies $x_0 = \Delta L z/h$. The surface of the slope is given by $F = x + x_0 = x + \Delta L z/h$. The kinematic boundary condition for a slope is

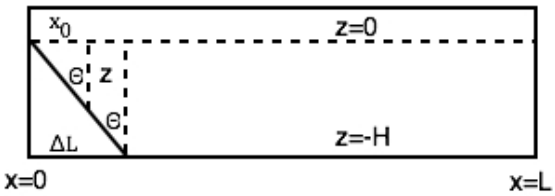

Figure 3: The notation used for a water tank with a slope at the left end

$$\frac{\partial F}{\partial t} + u\frac{\partial F}{\partial x} + w\frac{\partial F}{\partial z} = 0. \tag{40}$$

When the formula for the slope is inserted in the kinematic boundary condition, the lateral boundary condition for a slope is obtained:

$$u = -w\frac{\Delta L}{h}. \tag{41}$$

At x=0 and using $u = -\partial\phi/\partial x$ and $w = -\partial\phi/\partial z$ where ϕ is described by equation 25, the lateral boundary condition for a slope (equation 41) becomes

$$i(c^+ - c^-)\cosh[k(z+H)] = -\frac{\Delta L}{H}(c^+ + c^-)\sinh[k(z+H)]. \tag{42}$$

The space variable z is eliminated by integration over the water depth from -H to 0

$$i(c^+ - c^-)\int_{-H}^{0}\cosh[k(z+H)]\mathrm{d}z = -\frac{\Delta L}{H}(c^+ + c^-)\int_{-H}^{0}\sinh[k(z+H)]\mathrm{d}z \quad \Rightarrow$$

$$i(c^+ - c^-)\sinh[kH] = -\frac{\Delta L}{H}(c^+ + c^-)(\cosh[kH] + 1). \tag{43}$$

At x=L the water tank has a straight wall so the boundary condition used is

$$\left.\frac{\partial\phi}{\partial x}\right|_{x=L} = 0 \qquad \Rightarrow$$

$$i(c^+e^{ikL} - c^-e^{-ikL})\cosh[k(z+H)] = 0. \tag{44}$$

Which is integrated over the water height z to eliminate this variable

$$i(c^+e^{ikL} - c^-e^{-ikL})\int_{-H}^{0}\cosh[k(z+H)] \quad \mathrm{d}z = 0 \qquad \Rightarrow$$

$$i(c^+e^{ikL} - c^-e^{-ikL})\sinh[kH] = 0. \tag{45}$$

When equation 43 and 45 are solved, the constants of the velocity potential become $c^+ = 0$ and $c^- = 0$ which means no velocity potentiall ϕ exists. So for a water tank with a slope you need evanescent waves to solve the velocity potential, so in this topography evanescent waves are present.

2.5 The dispersion relation in a water tank with vertical walls

In section 2.4.1 is demonstrated that the wave number is $k = \pi n/L$ for a water tank with length L and vertical walls. In this expression n is an integer which corresponds to the order of the resonant wave. As shown in figure 4 if n is odd the waves have in the middle of the water tank a node, so the amplitude is minimal. For an even n, an antinode is located in de middle so the amplitude is maximal. The dispersion relation becomes for resonant frequencies:

$$\omega = \pm\sqrt{g\frac{n\pi}{L}\tanh[\frac{n\pi}{L}H]}. \tag{46}$$

The dispersion relation in the shallow water limit becomes for resonant frequencies:

$$\omega_n = \pm\sqrt{gH}\frac{n\pi}{L}. \tag{47}$$

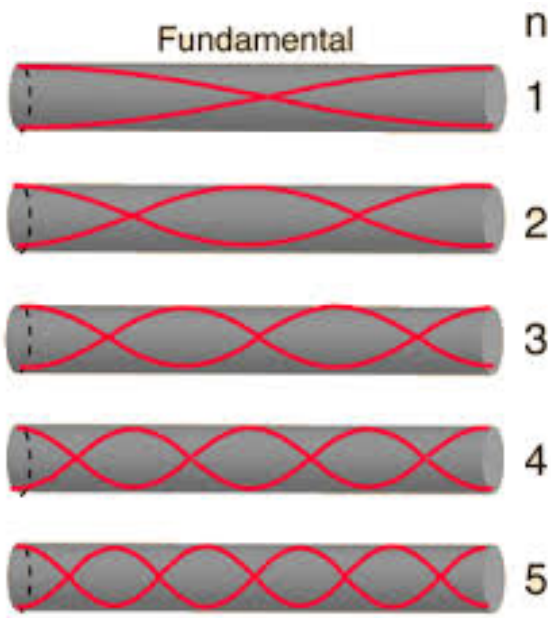

Figure 4: The first five resonant frequencies of a system with two closed ends [4].

3 Experimental setup

The quasi-1D experimental setup can be seen in figure 6. A water tank is located on a carriage. The interior measurements of the water tank are 198.0 ± 0.5 x 13.7 ± 0.1 x 26.0 ± 0.1 cm. The carriage is set horizontally in motion by a stepper motor with an amplitude of 5.0 cm. The stepper motor frequency is operated by the control panel, which tunes the frequency from 0.00 to 0.35 Hz in steps of 10^{-4} Hz. A red colouring agent is added to the water and a light source is placed behind the water tank for a better contrast between the water and the background. Different lengths of the water tank are created using vertical partitioning walls. These partitioning walls can be positioned perpendicular to the bottom of the water tank or with a tilt. Another way to change the topography of the tank is by adding one or more curved slopes. The dimensions of the slope are 23.0 ± 0.1 x 10.0 ± 0.1 x 16.0 ± 0.1 cm. The angle of inclination of the slope is between 13° and 40° with a mean inclination of 25.5°. Putting two slopes with their backs against each other a little mountain can be created as can be seen in figure 5. The length of the mountain can be increased by putting blocks with a width of 3 ± 0.1 cm, 5 ± 0.1 cm or 13.5 ± 0.1 cm between the slopes.

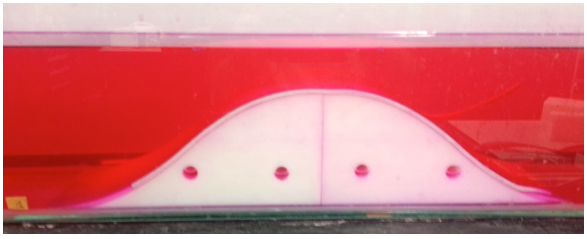

Figure 5: A mountain is created using two slopes.

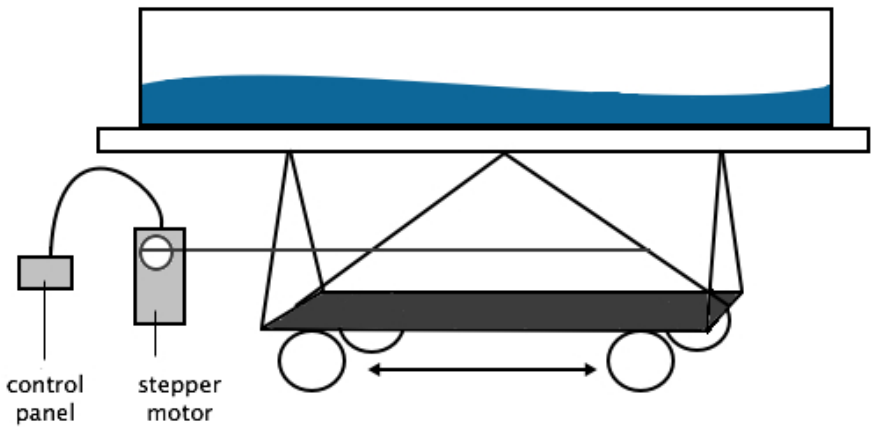

Figure 6: A schematic front view of the experimental setup. The stepper motion sets the carriage with the water tank in motion. The control panel tunes the stepper motor frequencies from 0.00 to 0.35 Hz.

The water tank movement is recorded by a camera. The camera is located approximately 6 meters from but at the same height as the water tank. A movie, consisting of separate images, is made with a capture speed of 8.0 frames/s using the image processing program 'Digiflow' [5]. This movie is read in Matlab, which results in images like figure7a. Next, the command 'edge' is used to determine the edges resulting in images like figure 7b, from which the water height in pixels can be determined. Afterwards the actual water height in centimeter is calculated for every x-position using the scale 1 pixel=$(8.1 \pm 0.2) \times 10^{-2}$ cm. This scale is determined by measuring the height of the water tank in centimeter and in pixels. When this is done for every frame, we end up with the water height as a function of place and time. The code for the data analysis can be found in the appendix 8.

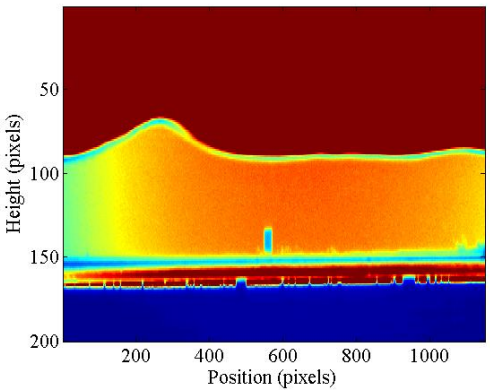

(a) Before the use of the command 'edge'.

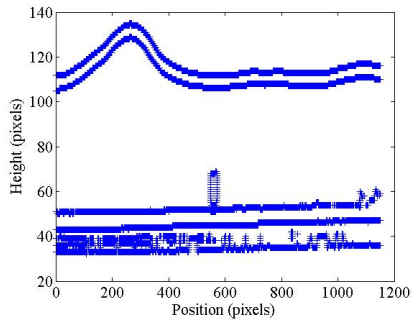

(b) After the use of the command 'edge'.

Figure 7: The water edge of the water tank for a water depth of 5.3 ± 0.1 cm continuously forced with a frequency of 0.2 Hz. A surface wave is visible at a position of about 300 pixels. The lines at the bottom of the picture are the bottom of the water tank and the edge of the surface on which the tank is standing.

3.1 Types of forcing

In this laboratory experiment different types of forcing are used:

Half oscillation The tank is moved from the far left to the far right or the other way around. This type of forcing is used to excite the first resonance wave, because in this way more water is to the left of the tank compared to the right, which gives rise to half a sine movement.

One oscillation The water tank is moved from the far left to the far right and back to the far left. It is also possible to do it the other way around, so starting at right. This type of forcing excites higher frequencies and inserts more energy in the system.

By hand using two plates To excite the higher resonant frequencies, the water has to be forced from both ends. This is done by moving two plates by hand 2 cm above the bottom from both ends towards the middle over a distance of 25 cm, which creates a burst of waves. A disadvantage of this type of forcing is that the energy in the system changes every time, because it is impossible to force the water with the same strength again by hand

Continuous oscillation The water tank is continuously forced. This method is used to create solitary waves. Most of the time the tank is oscillated for different forcing frequencies. The forcing frequency is decreased in steps of 0.002 Hz, starting at a high frequency where no solitary waves are visible. This 'high frequency' is different for each experiment. The forcing frequency can also be increased in the same steps starting from a low frequency, which also depends on the type of experiment.

4 Resonant waves

In this section is determined if the shallow water regime holds for resonant waves in a tank with vertical walls.

4.1 First resonant wave

The first experiment tests the dispersion relation in the shallow water limit (equation 47) for the first resonant wave (n=1). During this experiment a vertical partitioning wall was placed 51.5 cm from the right end of the water tank, which results in a water tank length of 146.5 ± 0.5 cm. The tank is forced half an oscillation from left to right in 2.5 ± 0.2 s. After this displacement the water height is recorded by the camera, from which the water height over time is determined 20 cm left of the vertical partitioning wall. This position is chosen because the first resonance wave has the highest amplitude near the end of the water tank. Close to the end of the water tank sometimes sloshing takes place, so 20 cm gives a more reliable measurement that is representative for the whole tank. Figure 8a shows the water height over time for a rest water depth of 7.3 ± 0.1 cm. In this figure the first resonant wave is seen, as well as damping. The resonant frequency is determined from the time difference between the peaks using $\omega = 2\pi/T$. For figure 8a the time difference T is 3.45 ± 0.05 s, which corresponds to a resonant frequency of $\omega = 1.82 \pm 0.03$ rad/s . The measured resonant frequency is in agreement with the theoretic resonant frequency in the shallow water limit of 1.81 rad/s.

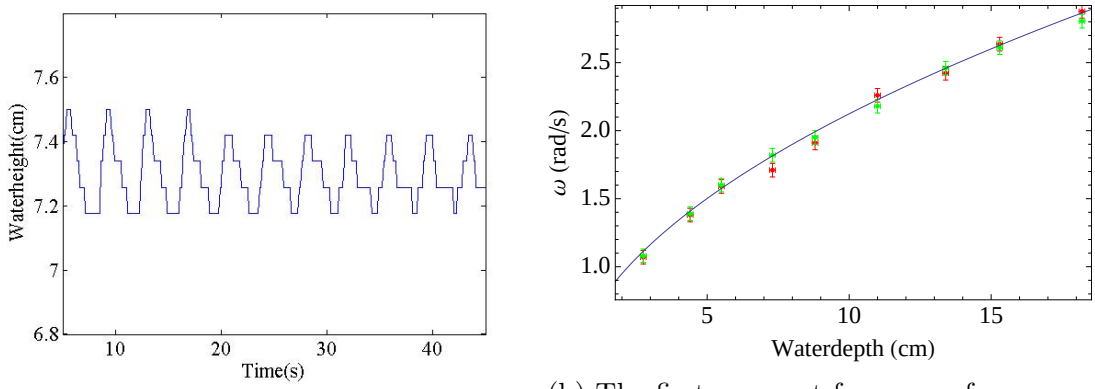

(a) The water height at 20 cm left of the vertical partitioning wall over time.

(b) The first resonant frequency for different water depths.

Figure 8: (a) The first resonance wave at a 20 cm left of the vertical partitioning wall over time is shown for a water depth at rest of 7.3 ± 0.1 cm. The frequency ω=1.82 ± 0.03 rad/s is measured from the time difference T=3.45 ± 0.05 s between the peaks. (b) The first resonant frequency for different rest water depths. The red and green points correspond to the measurements where the first resonant wave is excited using a forcing time of 2.5 ± 0.2 s and 3.3 ± 0.2 s respectively. Equation 47 for n=1 is plotted in blue, which is in good agreement with the measurements.

The first resonant frequency is measured for different depths with the method described above, using two different forcing times. The results are shown in figure 8b, where also equation 47 for n=1 is plotted in blue for different depths. The red and green points correspond to a forcing time of 2.5 ± 0.2 s and 3.3 ± 0.2 s respectively. The measurements fit the curve of dispersion relation in the shallow water limit, which means that the first resonant wave of the water tank is indeed in the shallow water limit regime.

4.2 Higher resonant waves

The next thing tested is if the shallow water limit also holds for higher resonant waves. To excite the higher resonant wave the water is forced by hand using two plates. A partitioning wall is added to the tank so the length of the water tank is 146.5 ± 0.5 cm. In figure 9a the change in water height over time can be seen for a water depth of 8.9 ± 0.1 cm measured 40 cm left of the vertical partitioning wall. It is hard to determine the resonant frequencies out of this signal, so the signal is reduced by the rest water depth whereafter the resonant frequencies can be found using fourier theory. The result of fourier theory is plotted in a *periodogram*, which is used to identify the dominant frequencies. On the y-axes of the periodogram the *power* is shown, which is not a physical quantity but a quantity used to indicate how strong the frequency is present in the signal. In figure 9b the periodogram of the waves at a water depth of 8.9 ± 0.1 cm can be seen in blue. The red bars are the theoretical resonant frequencies

predicted by equation 47. The first three measured resonant frequencies are in excellent agreement with the theortical frequencies. For higher frequencies the relation doesn't hold. This can be explained by looking at the wave length λ. The shallow water limit is also called the long wave limit. For higher frequencies the wave length becomes smaller, so the theoretical resonant frequencies for the longwave limit and measured resonant frequencies no longer coincide.

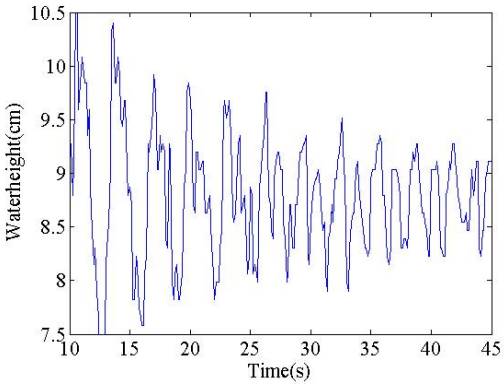

(a) The change in water height measured 40 cm left of the vertical partitioning wall.

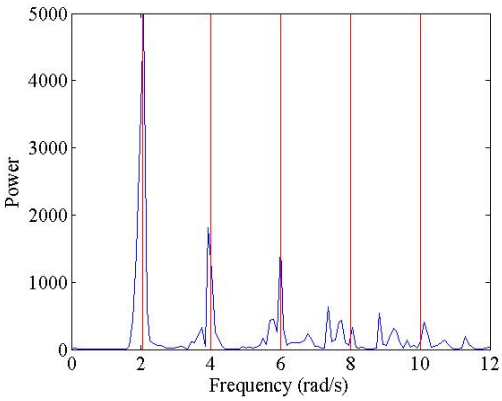

(b) The periodogram.

Figure 9: The water length is 146.5 ± 0.1 cm and the water depth is 8.9 ± 0.1 cm. The resonant frequencies of the waves in figure (a) are determined using fourier theory. The results are shown in a periodogram in figure (b) in blue. The red bars are the resonant frequencies predicted by equation 47. The first three resonant frequencies are in excellent agreement.

The frequencies are measured 40 cm left of the vertical partitioning wall, where up to 5 resonant waves are found. The resonant frequencies do not change with position, but at some positions not all modes are found because of nodes. This can be seen in figure 10 for a tank of length 146.5 ± 0.1 cm and for a water depth of 7.3 ± 0.1 cm. The periodogram in figure 10a is the result of a measurement at the right end of the water tank where the odd resonant frequencies dominate. Figure 10b is a result of a measurement in the middle of the water tank. The even resonant frequencies are dominant, because the odd frequencies have a node at the middle of the tank.

The higher resonant frequencies are excited at different water depth. The results of the fourier analysis for the waves at different depths are presented in figure 11. The lines are the dispersion relation in the shallow water limit plotted for different modes, starting at the first resonant frequency in red with n = 1 to the fifth resonant frequency in blue (n = 5). The points correspond to frequencies found using fourier analysis. They have the same colour as the corresponding mode. The 'normal' dispersion relation is

plotted as dashed lines.

The transition from the shallow water regime to the 'normal' regime is around a water depth of 12 cm. For smaller depths the measured frequencies follow the shallow water regime, but for higher water depths the 'normal' regime (dashed lines). An exception is the fifth resonant frequency in blue of which the measured frequencies for smaller depths as 12 cm are between the two regimes, which means the fifth resonant wave is never in the shallow water limit because of its small wave length. The reason the transition from the shallow water to the 'normal' regime is not visible in the previous section for the first resonant wave is because the regimes are close by each other for the first resonant wave.

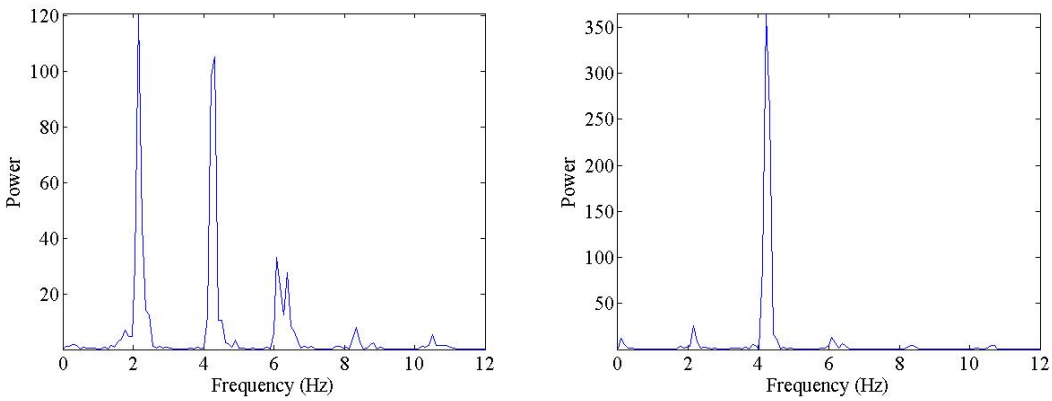

(a) Periodogram measured at the right end of the water tank.

(b) Periodogram measured in the middle of the water tank.

Figure 10: The water length is 146.5 ± 0.1 cm and the water depth is 7.3 ± 0.1 cm. At the end of the water tank the odd resonant frequencies are dominant. In the middle of the tank, the even frequencies are dominant, because odd frequencies have a node in the middle. The resonant frequencies do not change with position, but at some positions not all resonant frequencies are found because of nodes.

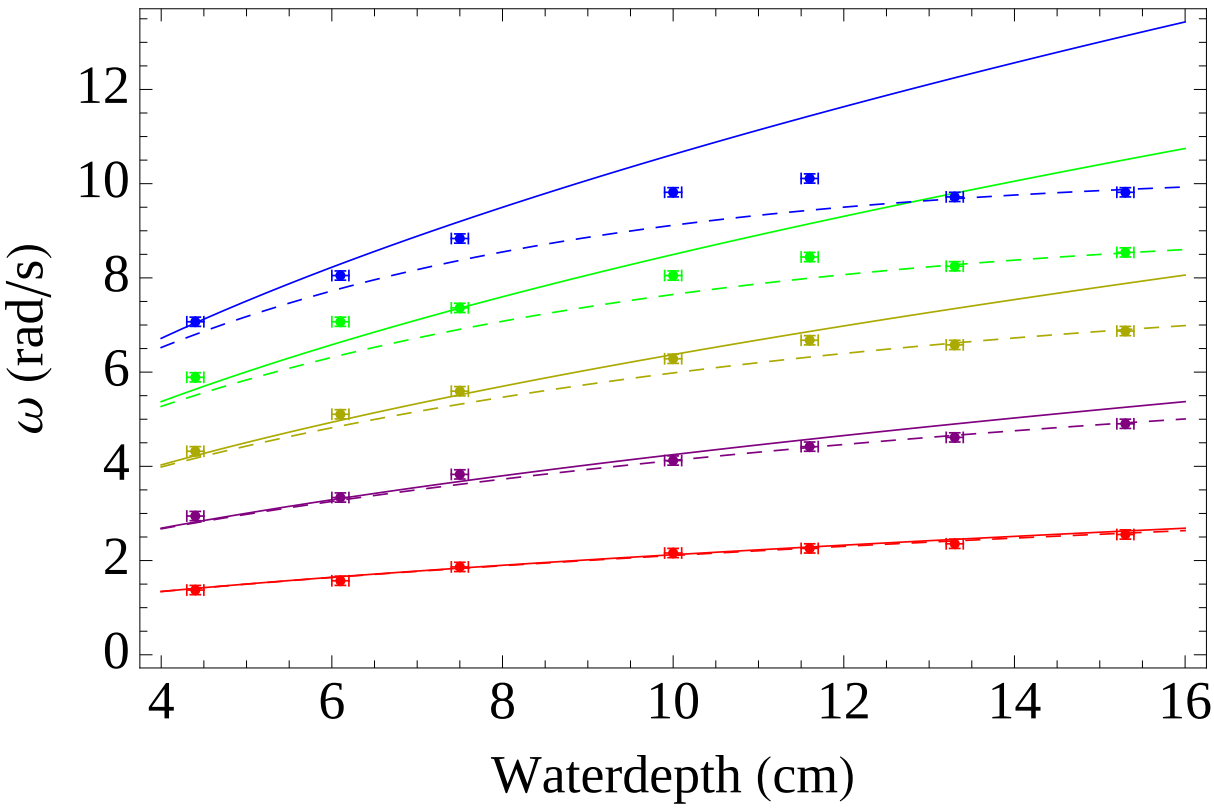

Figure 11: The first five resonant frequencies measured at different depths in a water tank length of 146.5 ± 0.5 cm. Equation 47 plotted in coloured lines for different modes, starting at n=1 in red to n=5 in blue. The dashed lines correspond to equation 46. The points are the frequencies found by fourier analysis of the waves measured at different depths.

5 Solitons

Solitons are solitary waves with a permanent form and constant velocity. When solitons cross each other they remain unaltered. [6] A soliton can exist on its own or with multiple solitons at the same time, which is called a soliton train. When the water tank is continuously forced at a high frequency, the system behaves like the first resonant wave: half a sine is observed. When the frequency is lowered all of a sudden one soliton is observed. Lowering the frequency results in more and more solitons, until the amplitude of the solitons becomes to small and the waves are damped. In figure 12 two solitons are shown moving from left to right at a water depth of 4.8 ± 0.1 cm and a water tank length of 188.0 ± 0.1 cm when the tank is continuously forced at a frequency of 0.206 Hz.

The emergence of solitons can be explained by the *Doppler shift*. When the tank is continously forced, the source (the water tank) moves with respect to the observer (the

wave). Waves propagating in one direction will see the wall of the tank moving towards them and cover less distance compared to the waves propagating into the other direction that see the wall moving away from them. The waves covering different distances results in a shift of the wave length and solitons emerge. The phenomenon of increasing number of solitons when the forcing frequency is lowered can be explained by the formula of the doppler shift. The formula of the doppler shift says that the observed frequency is inversely proportional to the velocity of the source, which means that if the forcing frequency increases the resonant frequency decreases. As the resonant frequency is proportional to the square root of the wave length will lowering the forcing frequency lead to a decrease in wave length. The horizontal length of the solitons ('wave length') decreases when more solitons appear.

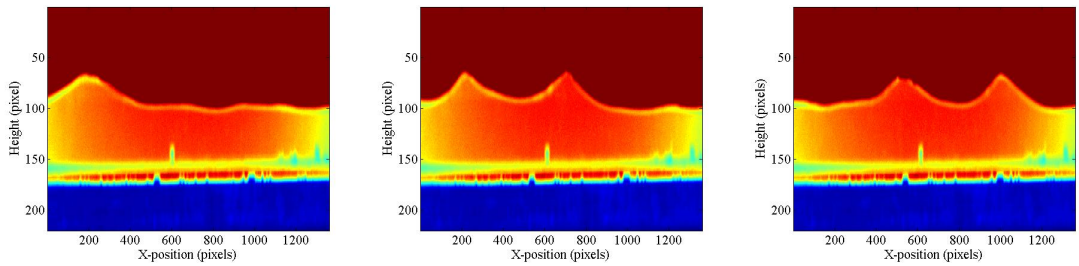

(a) t=0 s (b) t=0.375 s (c) t=0.75 s

Figure 12: Two solitons moving from left to right at a water depth of 4.8 ± 0.1 cm and a water tank length of 188.0 ± 0.1 cm when the tank is continuously forced at a frequency of 0.206 Hz. The shape of the solitons remains unaltered.

5.1 Hysteresis

Hysteresis is the history dependence of a system. Two or more equilibrium states are possible, depending on the behaviour of the system in the past. To demonstrate the hysteresis the water tank is continuously forced at a water depth of 5.3 ± 0.1 cm. Starting at 0.230 Hz the forcing frequency is *decreased* in steps of 0.002 Hz. After changing the frequency the number of solitons are counted after about 1 minute when a stable situation is reached. These measurements are shown in red in figure 13 in which the *frequency domains* of the solitons are plotted. The frequency domains are plotted as lines and for all the frequencies of one line the same number of solitons is measured. The blue points are the number of solitons starting at a frequency of 0.160 Hz and *increasing* the frequency in steps of 0.002 Hz.

At a forcing frequency 0.18 Hz two states are possible. When the forcing frequency is decreased from a high frequency (red) there are five solitons measured at 0.18

Hz. But when the forcing frequency is increased from a low frequency (blue) there are six solitons measured at 0.18 Hz. Two possible steady states depending on the historyof the system demonstrate the hysteresis.

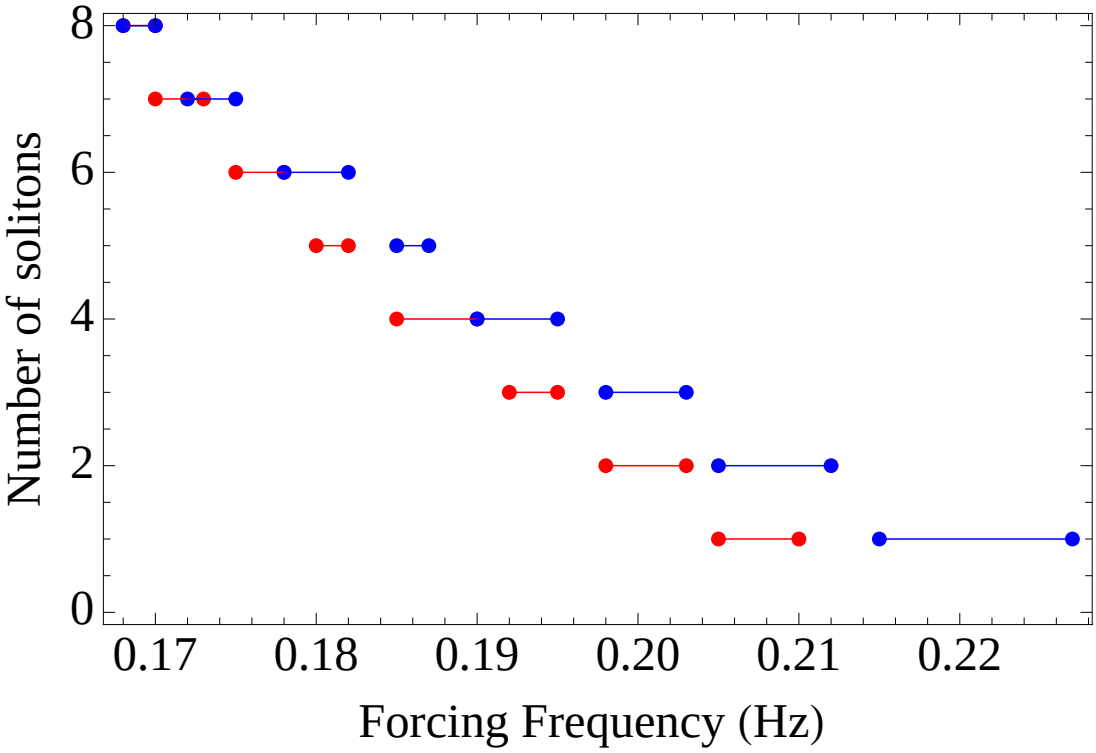

Figure 13: The number of solitons as a function of the forcing frequency. The red points are determined starting with a frequency of 0.230 Hz which is decreased in steps of 0.002 Hz. The blue points are determined starting with a frequency of 0.160 which is increased in steps of 0.002 Hz. Hysteresis is visible at e.g. 0.18 Hz for which 6 solitons are measured for starting with a low frequency and 5 solitons are measured for starting with high frequency.

5.2 The influence of the water tank length

To determine the influence of the water tank length on the frequency domains of the solitons, the water tank is continuously forced at a water depth of 4.7 ± 0.1 cm. Different lengths of the water tank are created by the vertical partitioning wall. The forcing frequency is decreased in steps of 0.002 Hz, starting at a high frequency where no solitons are visible which is different for each water tank length. After changing the frequency, the number of solitions is counted after about 1 minute when the situation is stable. In figure 14 the red, blue, green and yellow bars correspond to the frequency domains of a water tank length of 198.0 ± 0.5 cm, 168.0 ± 0.5 cm, 146.5 ± 0.5 cm and 127.0 ± 0.5 cm respectively.

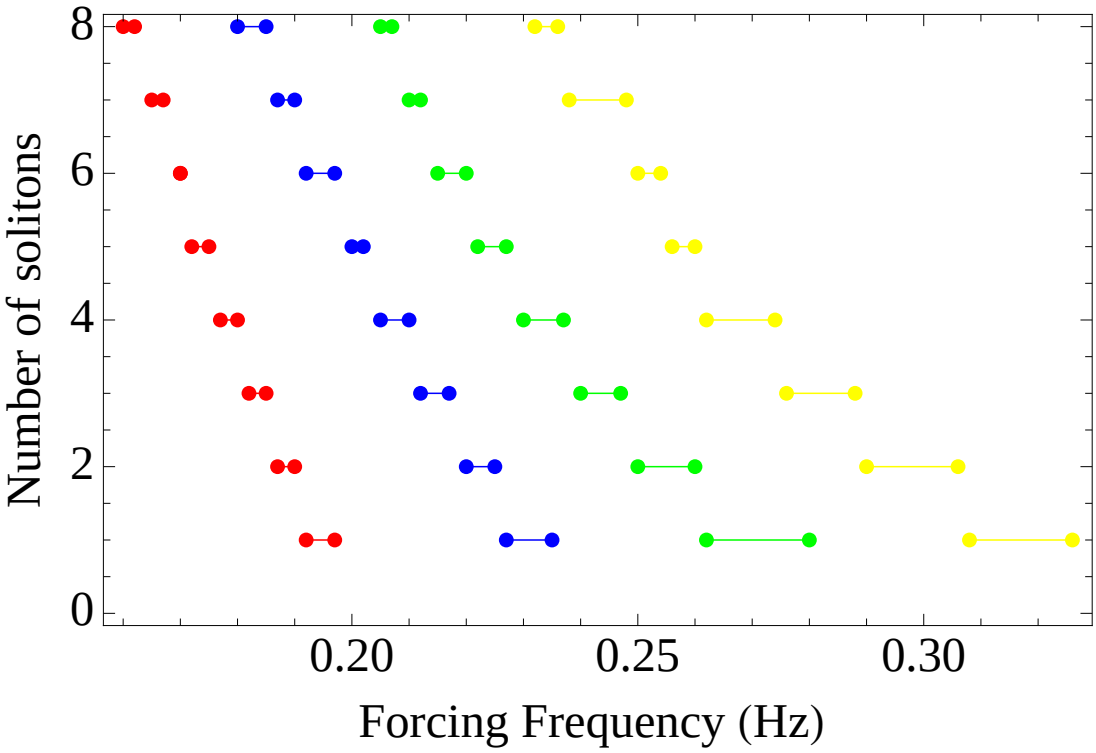

Figure 14: The influence of length on de frequency domains for the number of soiltons. The red, blue, green and yellow bars correspond respectively to a tank length of 198.0 ± 0.5 cm, 168.0 ± 0.5 cm, 146.5 ± 0.5 cm and 127.0 ± 0.5 cm. The width of the frequency domains increase with a decrease in length of the water tank. For a length of 146.5 ± 0.5 cm and 127.0 ± 0.5 cm the frequency domains get wider for smaller number of solitons.

In figure 14 the frequencies get higher when the length of the water tank becomes shorter. This can be explained by the dispersion relation which states that the frequency increases when the water tank length decreases, which can also be the reason that the frequency domains get wider when the water tank length decreases. Another possible explanation for the increase in the frequencies for a shorter water tank length is related to the Doppler shift. Solitons emerge because of waves going into a opposite direction cover different distances. This difference in distance stays the same for the different water tank lengths, but this difference becomes relative larger for a shorter water tank length which results in solitons emerging already at a higher frequency for shorter water tank length compared to larger water tank lengths.

For a water tank length of 146.5 ± 0.5 cm and 127.0 ± 0.5 cm (green en yellow) the frequency domains get wider for less number of solitons. For a water tank length of

127.0 ± 0.5 cm the length of the frequency bar for one soliton is $1.20 \cdot 10^{-2}$ Hz and for eight solitons $0.04 \cdot 10^{-2}$ Hz. This can be related to the 'crest-to-trough' excursion of the soliton, which decreases when the number of solitons increases. It could be that due to the decrease in the 'crest-to-trough' excursion of the soliton it is easier to form a new soliton, which leads to earlier formation of a new soliton when there are already more solitons. So the frequency domains get smaller for a higher number of solitons because new solitons are formed easier.

5.3 The influence of the water depth

The frequency domains of the solitons are also determined for different water depths. The water tank without a partitioning wall (L = 198.0 ± 0.5 cm) is continuously forced from a high frequency which is lowered in steps in 0.002 Hz. The frequency domains are shown in figure 15 where the red, blue, green and yellow bars correspond to a water depth of 4.7 ± 0.1 cm, 5.3 ± 0.1 cm, 6.2 ± 0.1 cm and 7.1 ± 0.1 cm respectively. The increase in frequency with increasing depth can again be explained by the dispersion relation that states that the frequency increases when the water depth increases, which is also a possible explanation for the increase of the width of the frequency domains with increasing water depth. For higher water depths the frequency domains also get wider for a smaller number of solitons, because it is easier to form new solitons for a higher number of solitons.

When the depth increases, both the 'crest-to-trough' excursion and the horizontal length of the soliton increase. In figure 16 the 'crest-to-trough' excursion is 5.0 ± 0.1 cm (62 pixels) and the length of the soliton is 55.0 ± 2.4 cm (679 pixels) for a water depth of 7.1 ± 0.1 cm. At a water depth of 5.3 ± 0.1 cm the 'crest-to-trough' excursion is 3.2 ± 0.1 cm (39 pixels) and the horizontal length of the soliton is 40.4 ± 1.0 cm (499) pixels. When the water depth is higher, there is more water available to the solitons which leads to an increase in the 'crest-to-trough' excursion and length of the soliton. The increase in the 'crest-to-trough' excursion and the horizontal length of the solitons can be another possible explanation for the increase of the width of the frequency domains with increasing water depth.

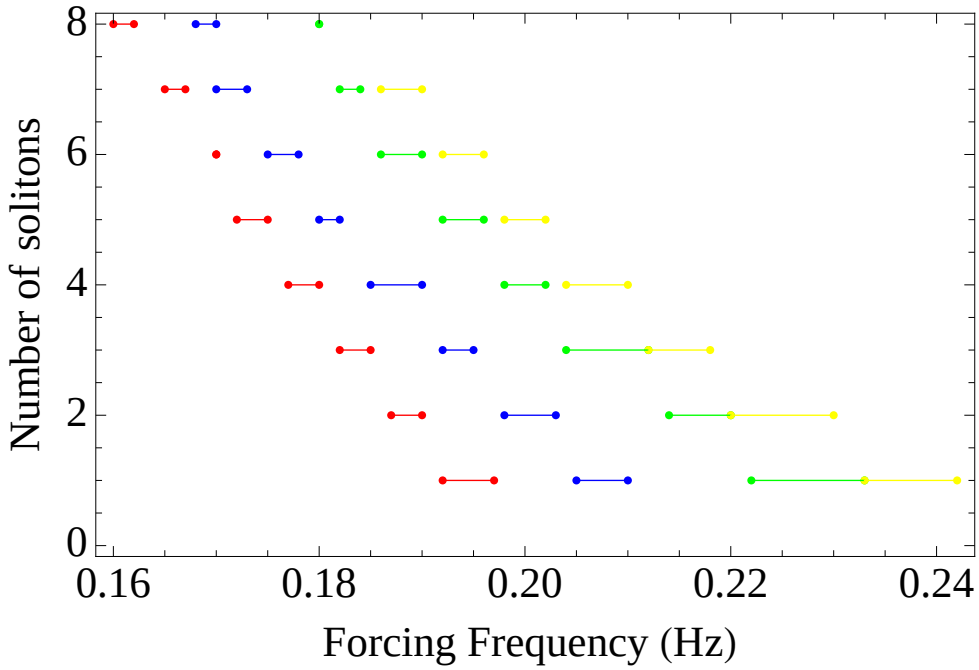

Figure 15: The frequency domains of solitons for different water depths. The red, blue, green and yellow bars correspond respectively to a water depth of 4.7 ± 0.1 cm, 5.3 ± 0.1 cm, 6.2 ± 0.1 cm and 7.1 ± 0.1 cm .The frequency domains become wider with increasing water depth and for higher water depths de domains get wider with decreasing number of solitons.

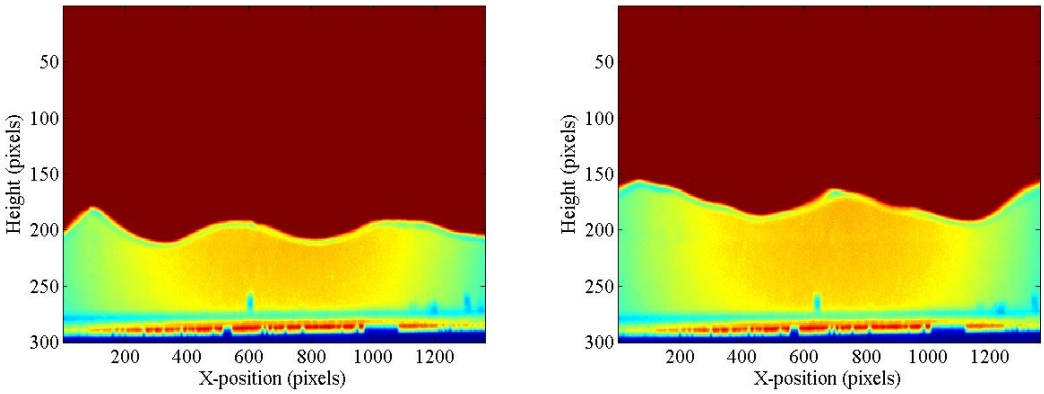

(a) Three solitons at a water depth of 5.3 ± 0.1 cm.

(b) Three solitons at a water depth of 7.1 ± 0.1 cm.

Figure 16: (a) At a water depth of 5.3 ± 0.1 cm 'crest-to-trough' excursion is 3.2 ± 0.1 cm (39 pixels) and the horizontal length of the soliton is 40.4 ± 1.0 cm (499) pixels. (b) At a water depth of 7.1 ± 0.1 cm the 'crest-to-trough' excursion is 5.0 ± 0.1 cm (62 pixels) and the length of the soliton is 55.0 ± 2.4 cm (679 pixels). Both the 'crest-to-trough' excursion and width of the soliton increase with increasing water depth.

6 Topography of the water tank

In this section the topography of the water tank is changed by placing the partioning wall at a tilt creating a tank with a slope as described in the theory in section 2.4.2. A change in the topography of the water tank is also accomplished by adding the slope and mountain of which the dimensions and angle of inclination are described in the experiment setup.

6.1 The partitioning wall at a tilt

The partitioning wall can be placed with a tilt. The angle of the tilt is measured in 'Digiflow' with a ruler, which uses the same convention as the unit circle to measure the angles as shown in figure 17. From the view of the left compartment for angles up to 90° the length of the water tank becomes larger. From equation 47 is expected that the resonant frequencies become smaller when the water tank increases. For angles larger than 90° the length of the water tank becomes smaller, so the resonant frequencies decrease.

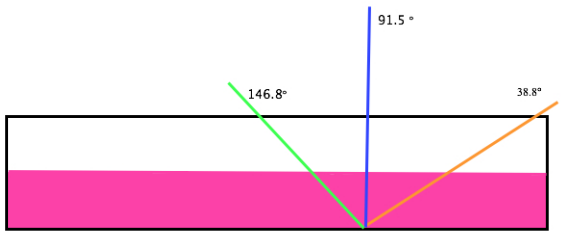

Figure 17: The angle convention used to measure the tilt of the partitioning wall.

In this experiment is the effect of a slope on the resonant frequencies determined. The partitioning wall is placed 51.5 ± 0.5 cm from the right end of the tank, so the tank length L is 146.5 ± 0.5 cm. The water tank is forced for one oscillation with a forcing time of 3.3 ± 0.2 s at a water depth of 7.3 ± 0.1 cm. The first three resonant frequencies are measured using fourier analysis for different tilts at 40 cm from the left end of the tank. In figure 18a is the frequency difference $\Delta\omega = f_{measured} - \omega_n/2\pi$ shown for the different angles of tilt where ω_n is the theoretical frequency from equation 47. The red points correspond to the first resonant frequency (n = 1), the green points to the second (n = 2) and the blue points to the third resonant frequency (n = 3). The difference $\Delta\omega$ becomes larger with increasing angle of tilt, which agrees with our expectation of larger resonant frequencies for larger angles. The difference $\Delta\omega$ also increases with the order of resonance n.

In figure 18b the periodogram is shown for three different angles of tilt. The colours orange, blue and green correspond respectively to an angle of tilt of 38.8°, 91.5° and 148.6°. The first two resonant frequencies can be seen around 2.16 Hz and 4.32 Hz. The third resonant frequency is theoretically predicted around 6.48 Hz, but a clear peak

is not observed. The frequency shift from the lowest resonant frequency corresponding to an angle of 38.8° to the highest frequency corresponding to an angle of 146.8° is again observed. There are no changes in the width of the peaks, but height differences between the peaks are observed. Particularly interesting is that for the first resonant frequency the height increases from 38.8° to 146.8° opposite from the second resonant frequency where the height decreases from 38.8° to 146.8°. So for angles smaller than 90° the second resonant frequency dominates and for angles larger than 90° the first resonant frequency dominates. This effect could be explained by the evanscent waves behaving different for angles larger than 90° compared to the angles smaller than 90° resulting in a different dominant frequency, but this is not tested in this thesis.

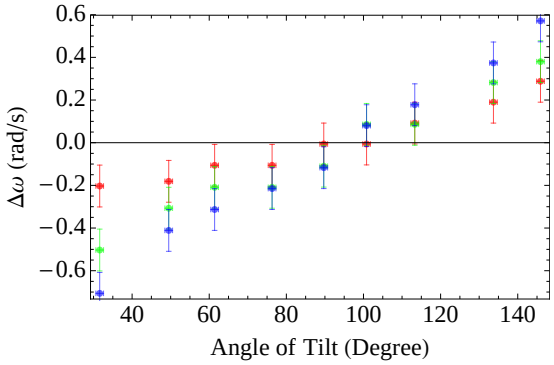

(a) The frequency difference $\Delta\omega = f_{measured} - \omega_n/2\pi$ for the different angles of tilt.

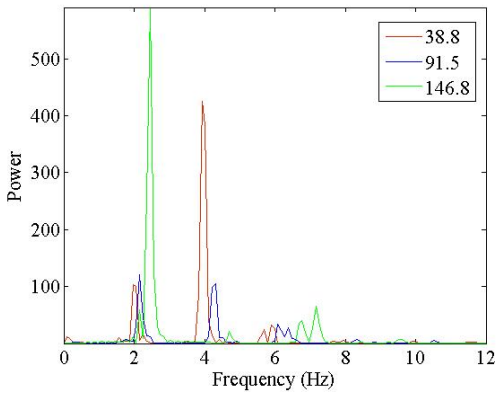

(b) The periodogram for the different angles of tilt.

Figure 18: In a water tank with length a water depth of 7.3 ± 0.1 cm a partitioning wall is placed with different angles of tilt 51.5 ± 0.5 cm from the right end of the tank leading to a tank length of approximately 146.5 ± 0.5 cm. (a) The red, green and blue points correspond to the first, second and third resonant frequency measured 40 cm from the left end of the tank. The frequency difference $\Delta\omega$ becomes larger with increasing angle of tilt and increasing order of resonance. (b) The colours orange, blue and green correspond respectively to an angle of tilt of 38.8°, 91.5° and 148.6°. The resonant frequency increases with larger angles of tilt. The width of the peaks do not change, but for angles smaller than 90° the second resonant frequency dominates and for angles larger than 90° the first resonant frequency dominates.

6.2 Changing the location of the mountain

The next topography change that is investigated is the mountain. When the mountain shown in figure 5 is put inside of the water tank it lowers the resonant frequencies. This is because the mountain decreases the water depth locally and the resonant frequency ω in equation 47 is proportional to $\sqrt{H}$, with H the water depth. How much the resonant

frequencies changes depends on the location of the mountain. The water tank is forced for one oscillation starting at the left with a forcing time of 3.3 ± 0.2 s. The mountain consists of two slopes with a total length of 42 cm. The first and fourth resonant frequency are measured 30 cm next to the end of the mountain using fourier theory. This is done for several locations of the mountain and for different water depths of which the results are shown in figure 19. The blue points correspond to water depth of 12.1 ± 0.1 cm, the red points to a depth of 13.1 ± 0.1 cm and the green points to a depth of 14.1 ± 0.1 cm. The location of the mountain is measured from the left end of the water tank to the middle of the mountain.

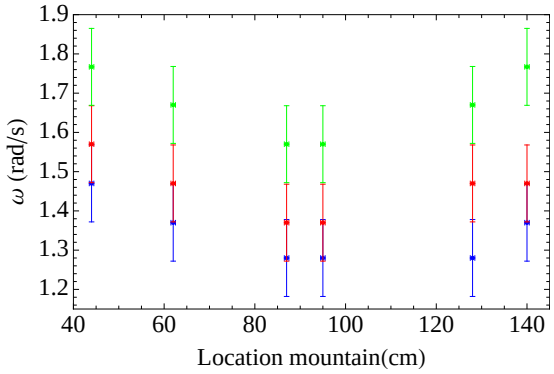

(a) The first resonant frequency for different locations of the mountain measured at three depths.

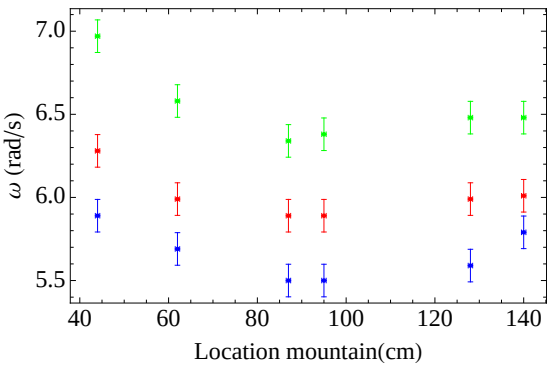

(b) The fourth resonant frequency for different locations of the mountain measured at three depths.

Figure 19: The first and fourth resonant frequency for different positions of the mountain for three water depths: 12.1 ± 0.1 cm in blue, 13.1 ± 0.1 cm in red and 14.9 ± 0.1 cm in red. The length of the mountain is 42.0 ± 0.1 cm and the location of the mountain is measured from the left end of the water tank to the middle of the mountain. The first and fourth resonant frequency decreases the most in the middle of the water tank. This effect does not depend on the water height.

The resonant frequency decreases the most if the mountain is placed in the middle of the water tank. This effect does not depend on the water height. A possible explanation is the presence of evanescent waves near the mountain, because the mountain exists of two slopes around which evanescent waves are present. When the mountain is placed near the end of the water tank there is still enough space for the propagating waves to propagate freely, but when the mountain is placed in the middle of the water tank the propagating waves are blocked in the middle of the tank by the evanescent waves of the mountain which results in a lower resonant frequency.

In figure 19b the fourth resonant frequency is decreased less than expected at the location of 140.0 ± 0.5 cm for all three depths. The expectation would be that the frequency increases when the mountain is moved away from the middle of the tank. For the blue points corresponding to a depth of 12.1 ± 0.1 cm this is happening, but for the two other depths there is almost no increase from the location of 128.0 ± 0.5 cm to 140.0 ± 0.5 cm. This effect is not symmetric, the fourth resonant frequency does increase at the left end. This antisymmetric behaviour can be caused by the evanescent waves which behave different at the right end of the tank compared to the left end of the tank. Evanescent waves can also explain why this behaviour is not visible at the first resonant waves. In the previous section is thought that evanescent waves cause a different dominant frequency depending on which side the slope is. It could be that the evanescent waves at the right end are dominant for even frequencies so only cause the antisymmetric behaviour at the fourth resonant wave. The antisymmetric behaviour can also be explained by the forcing which is from left to right. This cause can be tested by doing the same measurements again for a right to left forcing, which unfortunately is not done in this experiment.

The strongest decrease of the first resonant frequency in the middle of the tank raised a question about the location of the node of the first resonant wave. *Does the location of the node, which is normally in the middle of the water tank, also change with the location of the mountain*? At a water depth of 13.1 ± 0.1 cm the water tank is forced for half an oscillation in a time of 3.3 ± 0.2 cm. In figure 20 the blue points corresponds to a forcing from left to right and the red points to a forcing from right to left. For the different locations of the mountain a movie is made, from which the location of the node and the first resonant frequency is measured. The *node displacement* is the difference between the location of the node with and without a mountain. The node displacement is shown in figure 20a for different locations of the mountain, where zero node displacement indicates the location of the node without a mountain which is the same for left-right and right-left forcing. When the node is displaced to the left compared to a tank with no mountain, the node displacement is chosen to be negative. When the node is displaced to the right the node displacement is positive.

The expectation was a linear displacement oft the node with the position of the mountain, but the change in the location of the node is discrete. When the tank is forced from left to right (blue) the node changes instantly from approximately 8 cm to the left to approximately 16 cm to the right when the location of the mountain changes from 75 cm to 87 cm. The change in the location of the node is not symmetric when you compare the left-right forcing with the right-left forcing. When the tank is forced from left to right (blue) the jump in the location of the node is between 75 and 87 cm from the left end of the water tank, while by right to left (red) forcing the jump is between 50 and 60 cm from the right end. Another observation is the change of the location of

the node is larger to the right (positive) than to the left (negative). In figure 20b the first resonant frequency is plotted for left-right forcing (blue) and right-left forcing (red). The black line is the first resonant frequency without mountain, which is the same for left-right and right-left forcing. The first resonant frequency differs a bit between the two types of forcing but within uncertainty of the frequency. The lowering of the first resonant frequency is symmetric.

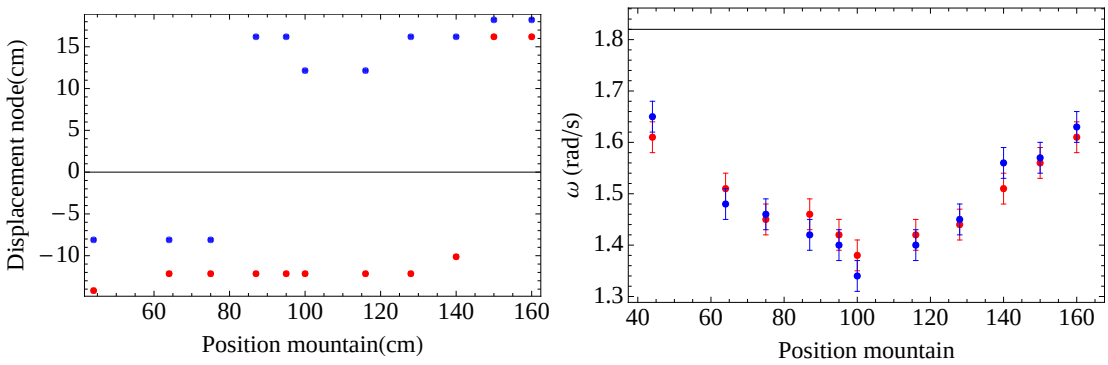

(a) The change of the location of the node for different locations of the mountain.

(b) The first resonant frequency for different locations of the mountain.

Figure 20: The blue and red points correspond to respectively left-right and right-left forcing (a) The zero line is the location of the node without a mountain. The node has moved to the left for negative values and to the right for positive values. The change in the location of the node is discrete and not completely symmetric for left-right and right-left forcing. (b) The black line is the first resonant frequency of the tank without the mountain. The lowering of first resonant frequency is symmetric and differs a bit between the two types of forcing but within the uncertainty of the frequency.

6.3 Changing the length of the mountain

Between the two slopes of the mountain blocks can be placed to change the length of the mountain. The first resonant frequency is measured for different lengths of the mountain using fourier theory and again for the three water depths of 12.1 ± 0.1, 13.1 ± 0.1 and 14.9 ± 0.1 cm. The middle of the mountain is placed 87.0 ± 0.5 cm from the left end of the water tank and the frequencies are measured 30 cm right of the mountain. When the length of the mountain increases, the first resonant frequency decreases. It looks like the frequency decrease is discrete, but this is because of the resolution of the frequency of the matlab program (0.098 Hz for a measured time of 35 seconds). The resolution Δf is improved by measuring for a longer period because $\Delta f = 2\pi/t$ where t is the measured time. But the waves are damped after a while so measuring for a long time will be of no use. Also the longer the measure time, the more data needs to be processed which takes unnecessary time. At a water depth of 12.1 ± 0.1 cm for a mountain length of 52 and

55 cm the resonant frequency was determined after measuring for 70 s, twice the normal time. The first resonant frequency changed from 1.18 ± 0.10 rad/s to 1.13 ± 0.05 rad/s. After increasing the measured time even more, no resonant frequencies are found because of the damping. Probably the lowering of the first resonant frequency will be continuous instead of discrete, but the resolution of the measured frequency of this set up is not high enough to determine it.

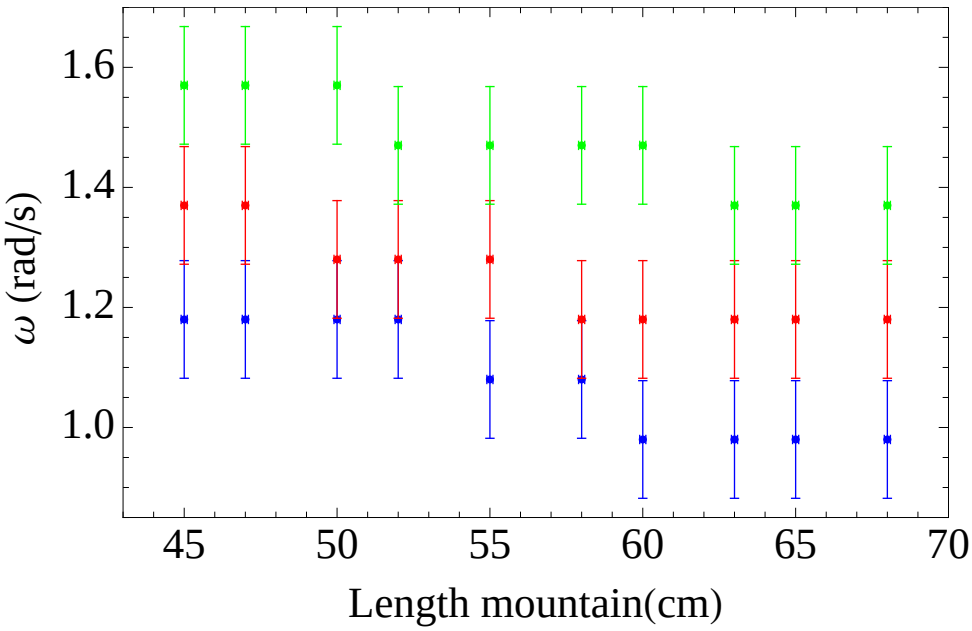

Figure 21: The first resonant frequency for different lengths of the mountain for three water depths: 12.1 ± 0.1 cm in blue, 13.1 ± 0.1 cm in red and 14.9 ± 0.1 cm in red. The middle of the mountain is placed 87.0 ± 0.5 cm from the left end of the water tank. The decrease in the first resonant frequency looks discrete due to the resolution of the measured frequency.

6.4 Continuously shaking with a slope

The last experiment shows the change in the frequency domains of the solitons and in the difference between the maximum and minimum surface elevation ΔH when a slope is added to the tank. The maximum and minimum surface elevation are the maximum and minimum water level of the whole tank during a measurement, which is different from the 'crest-to-through' excursion which is the difference between the maximum and minimum water level of one soliton. One half of the mountain is put at the right end of the tank. This setup is compared to the water tank with a vertical partitioning wall 10 cm from the right end to correct for the small decrease in water tank length due to the slope. The tank is shaken continuously starting at a high frequency which is lowered in steps of 0.002 Hz. After each step in frequency the number of solitons

are counted and a movie is made to determine the maximum and minimum surface elevation. These measurements are done for a water depth of 4.8 ± 0.1 cm and 6.3 ± 0.1 cm. The results are shown in figure 24 in which the red dots represent the water tank with the slope and the blue dots the water tank with the vertical partitioning wall.

As seen in figure 24a the maximum and minimum surface elevation do not differ between the slope and the partitioning wall at a water depth of 4.8 ± 0.1 cm. Likewise, no changes are seen in the difference between the maximum and minimum surface elevation ΔH, which is plotted in figure 24b. However when a slope is added to the water tank the frequency domains of the solitons, specified by the vertical lines, differ from the water tank with a vertical partitioning wall. The frequency domains coincide for six and seven solitons contrary to the domains of less solitons.

A difference in the 'crest-to-trough' excursion of the solitons moving to the left or to the right is observed for the water tank with the slope at a water depth of 4.8 ± 0.1 cm. When the solitons move away from the slope (left) the'crest-to-trough' excursion of the solitons is higher compared to moving towards the slope (right). This can be seen in figure 22 for a forcing frequency of 0.197 Hz. Because the 'crest-to-trough' excursion of the solitons is smaller, it sometimes appears with the eye like fewer solitons are moving to the right compared to moving to the left. Fortunately the matlab code was able to detect all solitons.

In figure 24c the number of solitons and the maximum and minimum surface elevation are shown for a water depth of 6.3 ± 0.1 cm. For low forcing frequencies the maximum and minimum surface elevation for the case with slope are almost the same as for the case with partitioning wall. But for higher frequencies the maximum/minimum surface elevation becomes larger/smaller for partitioning wall, which leads to a higher ΔH shown in figure 24d . An explanation for this observation is that the waves constructive interfere when they are reflected from a straight wall, but the interference pattern becomes more complicated when the waves are reflected from a slope.

When a slope is added at a depth of 6.3± 0.1 cm something unexpected is happening with the number of solitons, which is stated with 3* in figure 24c. The height of the slope is 10.0 ± 0.1 cm, so when the 'crest-to-trough' excursion of the solitons becomes too high water flows on top of the slope. Because of this process, three solitons move towards the slope (right) while only one solitons moves away from the slope (left) as can be seen in figure 23. This situation occurs until the 'crest-to-trough' excursion of the solitons becomes too low to flow on top of the slope and six solitons are visible.

At a water depth of 4.8 ± 0.1 cm the frequency domains for six and seven solitons coincide, in contrast to a water depth of 6.3 ± 0.1 cm where the frequency domain

for one soliton coincides. The frequency domains of the solitons were measured for starting with a low frequency as well as starting with a high frequency to determine the influence of the slope on hysteresis. At a water depth of 6.3 ± 0.1 cm for a water tank with the slope no hysteresis is observed, contrary to the water tank with the partitioning wall. At a depth of 4.8 ± 0.1 cm a little hysteresis is observed for the slope, but not as much as for the partitioning wall.

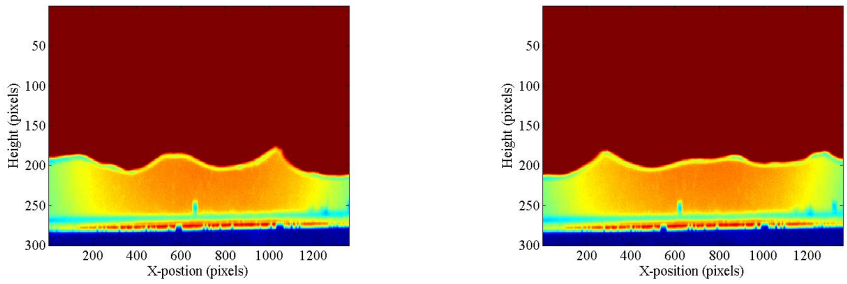

(a) Solitons moving to the right. (b) Solitons moving to the left.

Figure 22: A difference in the 'crest-to-trough' excursion of the solitons moving to the left or to the right is observed when the slope is added to the right-hand end of the tank at a water depth of 4.8 ± 0.1 cm. (a) The 'crest-to-trough' excursion of the solitons at a forcing frequency is 0.197 Hz from right to left are 2.92 ± 0.06 cm, 1.38 ± 0.03 cm and 1.62 ± 0.04 cm. (b) The 'crest-to-trough' excursion of the solitons at a forcing frequency is 0.197 Hz from left to right are 2.51 ± 0.06 cm, 1.30 ± 0.03 cm and 1.05 ± 0.03 cm. The solitons are higher when they move to the left end of the tank, so away from the slope.

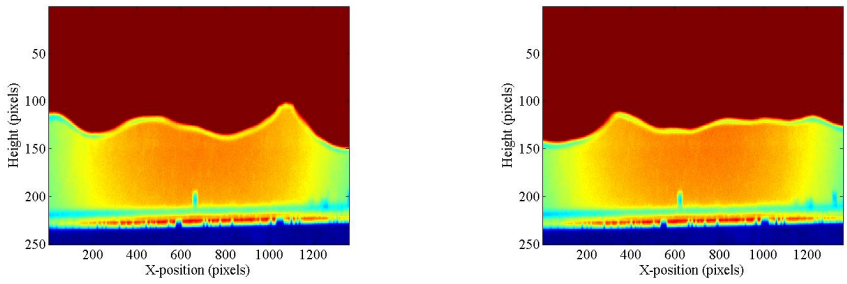

(a) Three solitons moving to the right at forcing frequency of 0.218 Hz. (b) One soliton moving to the left at forcing frequency of 0.218 Hz.

Figure 23: At a water depth of 6.3 ± 0.1 cm for a forcing frequency between 0.198 and 0.226 Hz there are three solitons moving to the right and one soliton moving to the left.

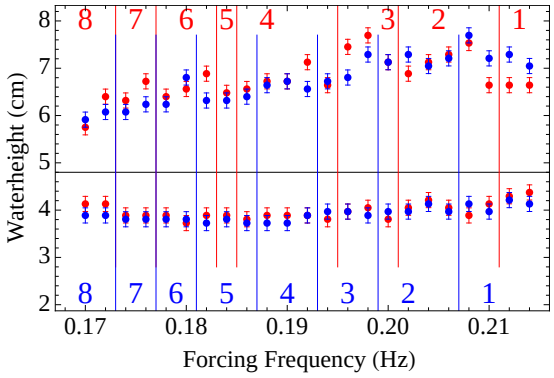

(a) The maximum and minimum surface elevation and the number of solitons for different forcing frequencies for a water depth of 4.8 ± 0.1 cm.

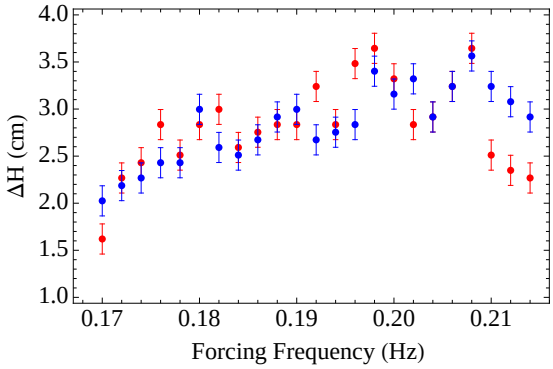

(b) The difference between the maximum and minimum surface elevation ΔH for different forcing frequencies for a water depth of 4.8 ± 0.1 cm.

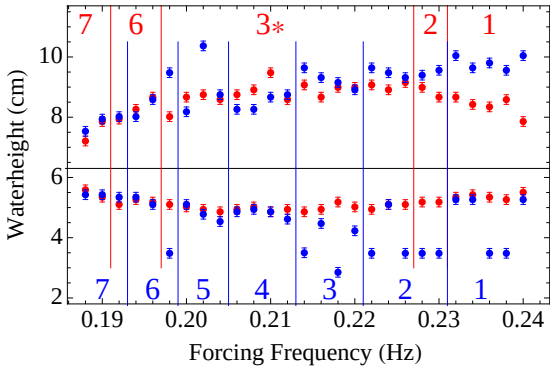

(c) The maximum and minimum surface elevation and the number of solitons for different forcing frequencies for a water depth of 6.3 ± 0.1 cm.

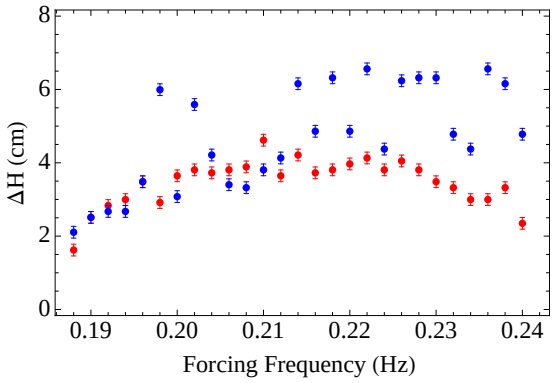

(d) The difference between the maximum and minimum surface elevation ΔH for different forcing frequencies for a water depth of 6.3 ± 0.1 cm.

Figure 24: Red corresponds to a water tank with a slope to the right. Blue corresponds to the water tank with a vertical partitioning wall 10 cm from the right end. For a water depth of 4.8 ± 0.1 cm the maximum and minimum surface elevation coincide for the slope and the partitioning wall, but the frequency domains of the solitons differ except for six and seven solitons. For a water depth of 6.3 ± 0.1 cm the maximum and minimum surface elevation coincide for low frequencies, but differ for higher frequencies. Also there are no three, four or five solitons visible when the slope is in the water tank, because the amplitude of the soltions is so big that water can flow on top of the slope. The number 3* corresponds to three solitons moving towards the slope (right) and one soliton moving away from the slope (left).

7 Discussion and conclusion

In this thesis laboratory experiments were done to determine the influence of the water depth, forcing frequency and topography of the water tank on surface waves and resonant frequencies.

Water depth
The influence of the water depth on the resonant frequencies was tested for the first five resonant frequencies and combined with the dispersion relation. A transition from the shallow water limit to the normal regime was observed for the resonant waves around a water depth of 12 cm. The influence of the water depth on solitons was also determined. An increase in the 'crest-to-trough' excursion, the horizontal length and the width of the frequency domains of the solitons for a increasing water depth was found. Also for higher water depths the frequency domains got wider for a smaller number of solitons.

Forcing frequency
Different types of forcing were used which all gave rise to different types of surface waves. The forcing type 'half oscillation' only excited the first resonant wave. 'One oscillation' and 'by hand using two plates' excited also the higher resonant waves. 'Continuously forcing' resulted in solitons of which the number depended on the forcing frequency. The hysteresis demonstrated the influence of the starting frequency, because a different amount of solitons was observed for starting at a high frequency compared to starting with a low frequency.

Topography of the water tank
The innovating topic of this thesis is the change in the topography of the water tank. This was done by changing the water tank length, putting the partitioning wall at a tilt and adding a slope or mountain. This manner of experiments was for the first time done at the NIOZ. The influence of the water tank length was only tested for solitons. The width of the frequency domains increased for decreasing water tank length and for smaller tank lengths the width increased with a smaller amount of solitons. The influence of the partioning wall with a tilt on the resonant frequencies was found to be increasing the resonant frequencies with increasing angle of tilt and with increasing order of resonance. For angles smaller than 90° the second resonant frequency dominated and for angles larger than 90° the first resonant frequency dominated, which could be caused by evanescent waves. Adding a mountain to the water tank lowered the resonant frequencies. These decreased the most in the middle of the water tank. This effect was further examined by looking at the change in the location of node for the first resonant frequency, which was found to be discrete and not symmetric contrary to the expectation of a linear and symmetric change. The influence of increasing the width of the mountain on the resonant frequencies looked discrete due to the resolution

of the measured frequency. The last topography change of which the influence was determined is the influence of the slope on the frequency domains of the solitons and the surface elevation by continuously forcing. For a small water depth no change in surface elevation was observed, but at a higher depth the surface elevation became larger for high forcing frequencies because of more constructive interference when the solitons are reflected on a straight wall compared to a slope. The frequency domains of the solitons also changed when the slope was added to the tank but no clear pattern was observed.

Limitations and future research

The forcing type 'by hand using two plates' is not a very exact method because it is hard to move the plates with the same force over exactly the same distance for a second time. The higher resonant waves are excited and these frequencies do not depend on the force and the distance as long as there is enough energy for the waves to propagate. The quantity power which is used to determine the dominant frequencies is related to how much energy is put in the system and changes every time when this type of forcing is used. In section 4.2 it is not possible to compare the resonant frequencies at different depths on the base of power. It would be nice if it is possible to determine which resonant frequency (first, second, third, etc.) is the dominant frequency at which depth. This problem was noticed after the measurements for the section about higher resonant frequencies, so from that moment on the method of a whole oscillation is used to measure higher resonant frequencies. For this type of forcing it is possible to compare dominant frequencies as done in section 6.1.

When the tank is continuously forced for water depths above 10.0 cm, the water is sloshed over the sides of the water tank which makes no experiments with a high water depth and continuously forcing possible with this setup. This types of experiments would be particularly interesting in cases with the slope or mountain. In the case of continuously shaking with a slope it would be nice to look what will happen with the number of solitons and the surface elevation if the slope is completely under water. Also it would be nice to look at the number of solitons and the surface elevation for a water tank with a mountain, which is only possible if the water depth is higher than the mountain. This problem can easily be solved by using a higher water tank.

A limitation in the data analysis is the resolution in the measured frequency after fourier theory, which makes the decrease in the frequency in section 6.3 look discrete. A linear decrease in the frequency is expected which can hopefully be proved with another setup that has a higher resolution of the measured frequency. Another limitation of this set-up is that only horizontal forcing is possible. Vertical forcing is necessary to excite one individual even resonant wave. Like it is done in section 6.2 for the node of the first resonant wave it would be interesting to look how the nodes for higher resonant frequencies change with the location of the mountain. Another interesting topic for

future research is to look for evanescent waves at the partitioning wall at a tilt or at the mountain. It would be useful to investigate if evanescent waves are indeed the cause of different dominant frequencies for different angles of tilt and the greatest decrease of the resonant frequencies when the mountain is placed in the middle.

8 Appendix: matlab code

The movie made with the camera is read in with the use of the function df_dfi_read in matlab. As explained in the experimental setup is the command 'edge' used to determine the water height. With the use of peakfinder the frequency is determined for the first resonant wave.

```
%height of waterlevel
file1=fopen('heg.dat','w');
for j=1:length(files)
    Str= df_dfi_read(fullfile(myFolder,files(j).name));
    I = Str.image.data(xmin:xmax,ymin:ymax);
    BW = edge(I, 'log');
    [row,col] = find(BW);
    lijn=col(find(row==800));
    height=max(lijn)-h;
    fprintf(file1,'%d %d\n', j, height);
end
fclose(file1);

load heg.dat
f1= heg(:,1);
hg = heg(:,2);
peak=peakfinder(hg);
last=length(peak);
period=(peak(last)-peak(2))/((last-1)*fs)
frequency=2*pi/period
```

The higher resonant frequencies are determined using fourier theory. The fast fourier transform is a standard function of matlab. The power is used to determine the dominant resonant frequencies.

```
%De-mean
mhg=hg-mean(hg);
fs = 8;

%Fast Fourier Transform
m = length(mhg);            % Window length
n = pow2(nextpow2(m));      % Transform length
f = (0:n-1)*(fs/n);         % Frequency range
```

```
y = fft(mhg,n);                % DFT
y0 = fftshift(y);              % Rearrange y values
f0 = (-n/2:n/2-1)*(fs/n);      % 0-centered frequency range
power0 = y0.*conj(y0)/n;       % 0-centered power
peak=peakfinder(power0,(max(power0)-min(power0))/32);

%Power
for i=1:length(peak)
    w=f0(peak(i))*2*pi;        %frequency in rad/s
    ph=power0(peak(i));        %power
    fprintf('%d %d\n', w, ph)
end
```

The last piece of code is used for analyses of the solitons. The number of solitons and the maximum and minimum surface elevation are determined.

```
%edge
file1=fopen('pos.dat','w');
file2=fopen('npmwl.dat','w');
for j=1:length(files)
    Str= df_dfi_read(fullfile(myFolder,files(j).name));
    I = Str.image.data(xmin:xmax,ymin:ymax);
    BW = edge(I, 'log');
    [row,col] = find(BW);

    %positions edge
    XY = zeros(xmax-xmin,2);
    for i=2:xmax-xmin
        place = find(row==i);
        list = col(place);
        mx = max(list);
        height = mx-h;
        XY(i,1) = i;
        XY(i,2) = height;
    end
    XY(1,1)=1;
    XY(1,2)=XY(2,2);

    %position peaks
    x = XY(:,1);
    y = XY(:,2);
    maxwl=max(y);
    mwl=min(y);
%minimum water level
    peak=peakfinder(y,(max(y)-min(y))/8,hw-h,1);
%position of the peaks
    nop=length(peak);
%number of peaks
```

```
    if mwl<20
        mwl=60;
    end

    %height of peaks
    if peak >0
        for i=1:nop
            hop=y(peak(i));
            fprintf(file1,'%d %d %d \n',j,peak(i),hop);
        end
    end

    if  nop>=2
        nump=nop;
        for i=1:nop-1
            npn=nump;
            if  peak(i+1)-peak(i)>75
                nump=npn;
            else nump=npn-1;
            end
        end
    else nump=nop;
    end

  fprintf(file2,'%d %d %d\n',j,maxwl,mwl); fprintf(file2,'%d %d %d\n',j,nump,mwl);
end
```

References

[1] S. Haver. Freak wave event at draupner jacket 1 january 1995. *Statoil, Tech. Rep*, PTT-KU-MA, 2003.

[2] J.M. Walker. Farthest north, dead water and the ekman spiral. *Weather*, 46.4: 103-107, 1991.

[3] B. Le Méhauté. *An introduction to hydrodynamics and water waves*. Springer-Verlag, 1976. ISBN 0-387-07232-2.

[4] R. Nave. http://hyperphysics.phy-astr.gsu.edu/hbase/waves/opecol.html harmonics of open air column.

[5] S.B. Dalziel. *DigiFlow users' guide, advanced image processing for fluid mechanics*. Dalziel Research Partners, Cambridge, 2009.

[6] M. Remoissenet. *Waves called solitons: concepts and experiments*. Springer, 3rd edition, 1999. ISBN 978-3-662-03790-4.